Theory of Coherent Population Trapping in Warm Hydrogen Plasmas in Weak Magnetic Fields

James M. Mitrani

7/29/09

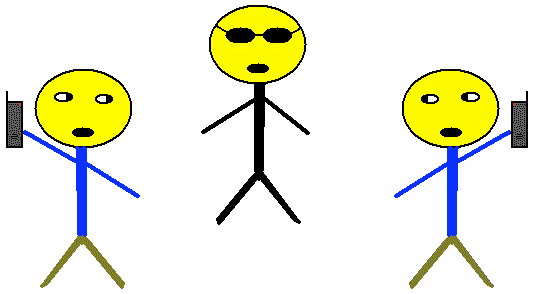

Thanks!!!

- Thanks to G-d!
- Also, thanks to Dr.'s Cohen, Farley, Jau, Foley, Levinton, and other faculty and students who helped me with this project.
- Also, thanks to the PPPL PPST, Princeton University, and other institutions for their support.

Goal

- The goal of this project is to describe a plasma diagnostic that uses coherent population trapping (CPT) to measure low strength (<250 G) magnetic fields in plasmas. Understanding **B**-fields is critical for MCF.
- This diagnostic will be tested in the Princeton field-reversed configuration (PFRC).

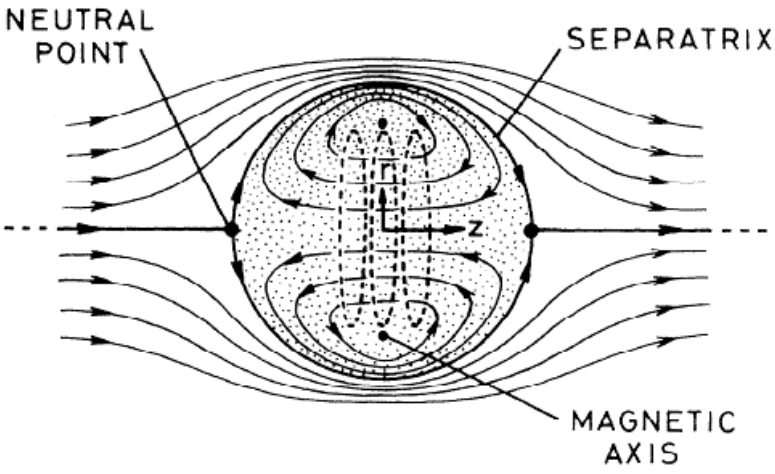

FRC magnetic field lines. The plasma is confined in the central (circular) region of the FRC. The solid, closed lines in the center of the FRC represent the poloidal field lines which confine the plasma. The dotted lines represent possible toroidal field lines, which are present in a spheromak, but absent in an FRC. Figure courtesy of [Hugrass, *J Plasma Phys.* **26** (1981)].

FRC model fields: which is produced experimentally?

I. Hill's vortex, Rigid rotor (Solov'ev)

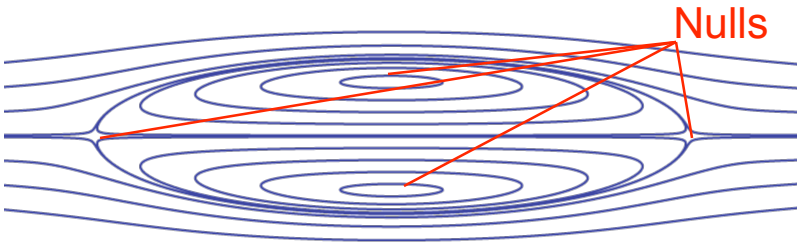

II. RR: odd-parity (Cohen, Milroy)

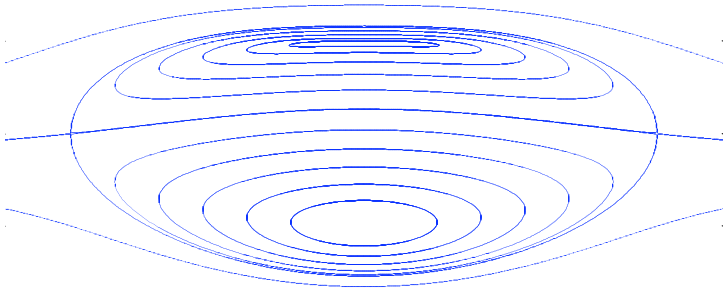

III. RR: discrete FCs

(Meyers, Kornack, Cohen)

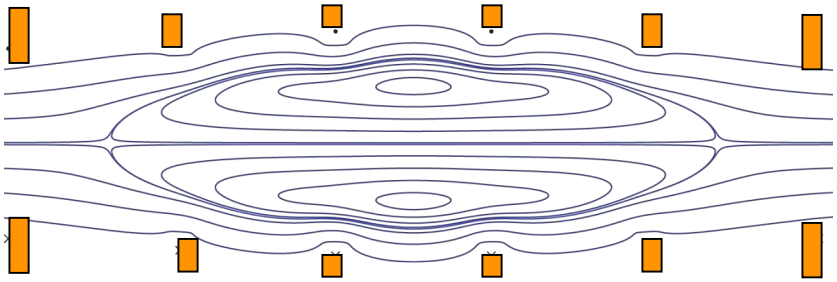

IV. Hybrid: RMF_0 (Belova)

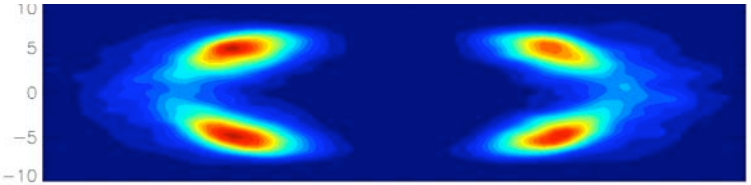

V. PIC: RMF_o, Discrete FCs

(Welch, Cohen)

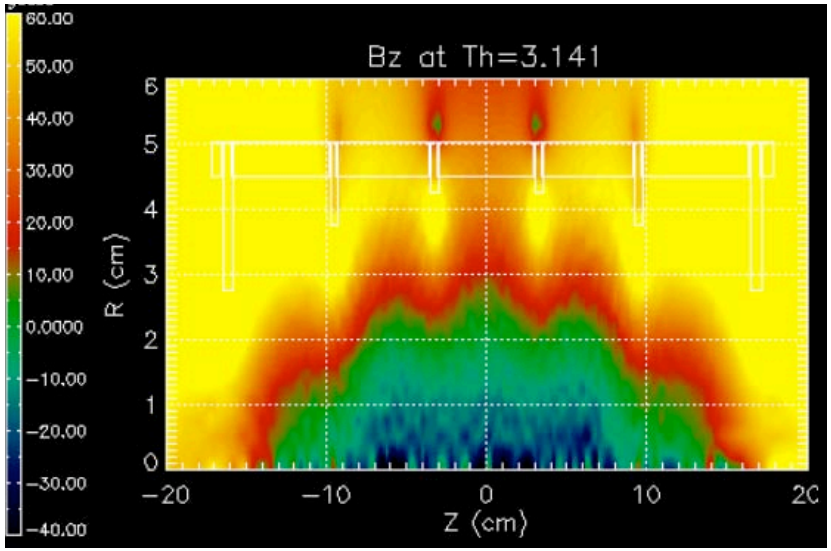

Other Means for Measuring B

- Other diagnostics include: Probes, MSE, MSE-LIF, DSI, optical magnetometers…
- In hotter devices, probes will melt. MSE has been successful for measuring strong fields.
- Best approaches are minimally invasive.

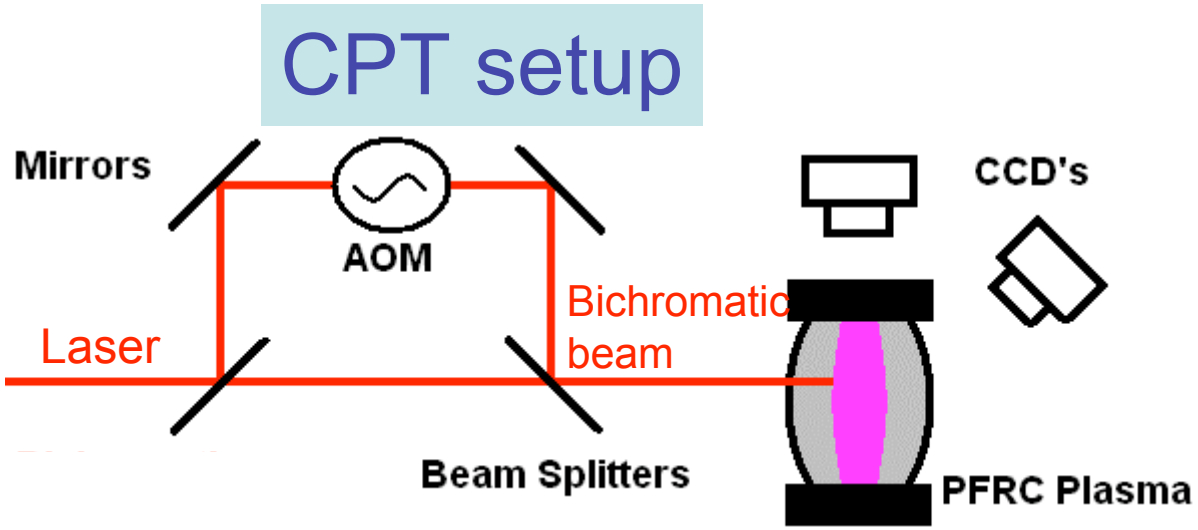

Outline

- Theory of coherent population trapping. How one can use CPT to measure **B**-fields in plasmas.
- Building an **exhaustive** model of CPT using the appropriate parameters from this experiment.
- Measuring fluorescence and the **B**-field from CPT effects.
- Clarifying assumptions, future experiments, and summary of results.
  - First extensive CPT model on hydrogen. (Isidor Rabi preferred working with hydrogen!)
  - First to show that CPT effects can be observed on the H_α line, even accounting for various spectroscopic complications.

Outline

- Theory of coherent population trapping. How one can use CPT to measure **B**-fields in plasmas.
- Building an exhaustive model of CPT using the appropriate parameters from this experiment.
- Measuring fluorescence and the **B**-field from CPT effects.
- Clarifying assumptions, future experiments, and summary of results.
  - First extensive CPT model on hydrogen. (Isidor Rabi preferred working with hydrogen!)
  - First to show that CPT effects can be observed on the H_α line, even accounting for various spectroscopic complications.

CPT – Assertion

- The “textbook” approach to explain CPT involves two lasers and a Λ-system (**b**).
- In a 2-state system (**a**), a laser will pump atoms from the ground state to the excited state. The effectiveness of pumping is maximized when $\omega_L=\omega_E-\omega_G$ ($\delta_L=0$); the laser is resonant with the transition.
- In the Λ-system, define δ_R as the Raman detuning parameter. When $\delta_R=0$, the atoms are trapped in a superposition of the ground states, and the excited state population surprisingly depletes. This is the essence of CPT and overcomes Doppler broadening!

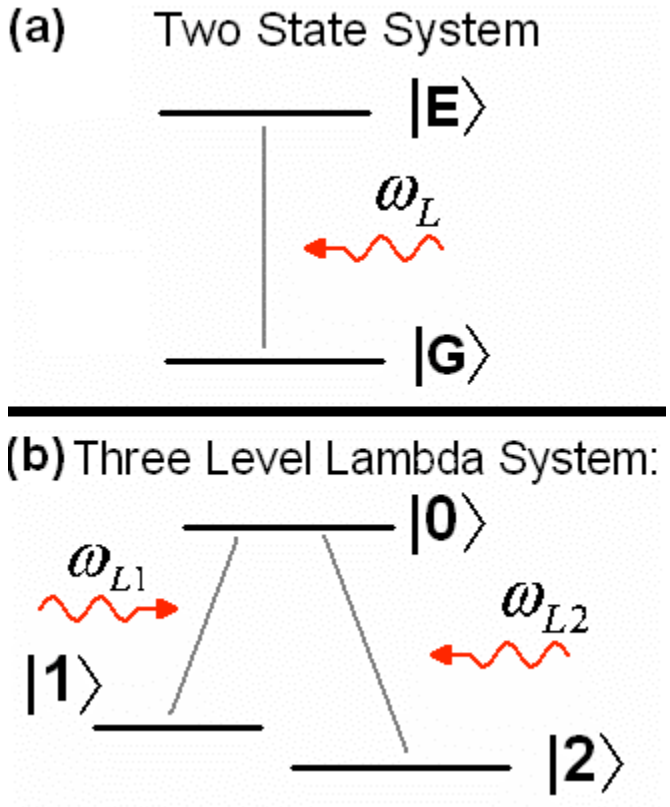

*** Raman detuning parameter ***

$$\begin{aligned}\delta_R &= \delta_{L1}-\delta_{L2}\\ &= \left(\omega_{L1}-k_1 v_T-(\omega_0-\omega_1)\right)-\left(\omega_{L2}-k_2 v_T-(\omega_0-\omega_2)\right)\\ &\cong \omega_{L1}-\omega_{L2}+\omega_{12}\end{aligned}$$

CPT – Explanation

- Physically, when the lasers have appropriate frequencies and phases, the atoms are trapped in a superposition of the states *1* and *2*.
- To observe CPT, fix ω_{L2} at resonance with the transition between states *0* and *2*, and scan ω_{L1} around its resonance frequency.
- As $|\delta_R|$ gets smaller, optical pumping is more effective. But when $\delta_R=0$, the upper-state population rapidly depletes.
- From the Zeeman effect, one can measure the magnetic field strength.

(Right): Upper-state steady-state population resulting from laser scanning.

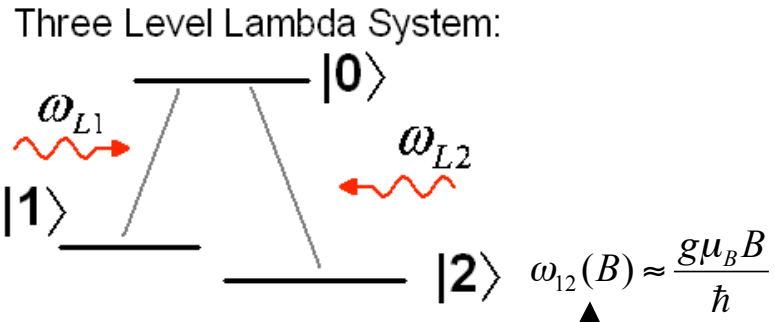

Zeeman splitting (in the ground states) is a function of the external magnetic field.

$$\delta_R = \omega_{L1} - \omega_{L2} + \omega_{12}$$

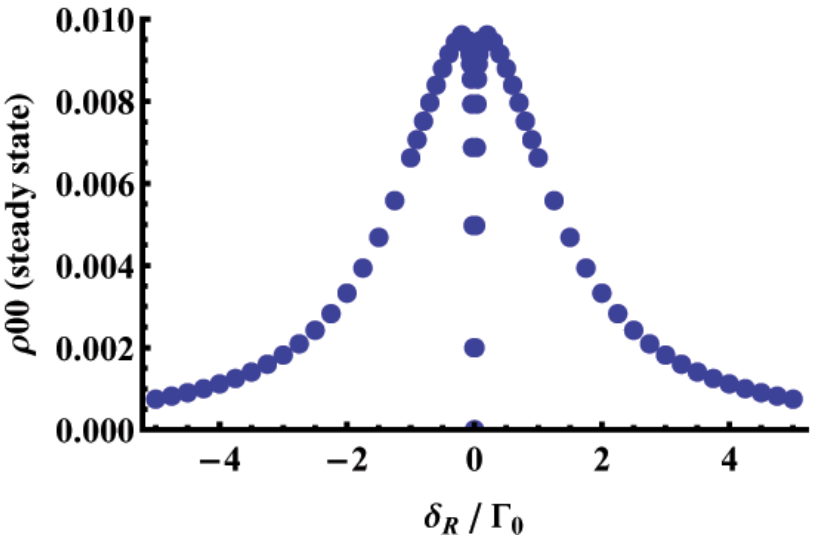

CPT – Derivation

- CPT can be derived from the Bloch equations:

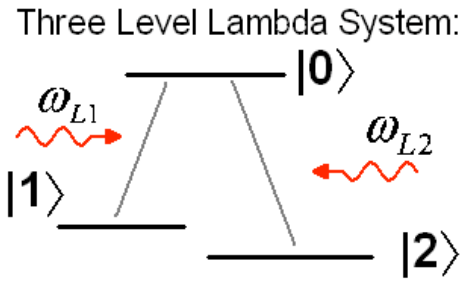

$$\frac{d}{dt}\rho = -\frac{i}{\hbar}\left[H_0 + H_1, \rho\right] + \Re\rho$$

Density Matrix

$$\begin{pmatrix} \rho_{00} & \rho_{01} & \rho_{02} \\ \rho_{01}^{*} & \rho_{11} & \rho_{12} \\ \rho_{02}^{*} & \rho_{12}^{*} & \rho_{22} \end{pmatrix}$$

Hamiltonian w/o Lasers:

$$H_0 = \hbar \sum_{j=0}^{2} \omega_j \left| j \right\rangle\left\langle j \right|$$

Phenomenological Rate Operator

Interaction Hamiltonian (dipole transition):

$$H_1 = \sum_{k=1}^{2} \frac{\hbar\Omega_{Rk}}{2} \exp[-i(\omega_{Lk}t + \delta\phi_k)] \left| 0 \right\rangle\left\langle k \right| + h.c.$$

CPT – Derivation

Solving the Bloch equations yields six differential equations:

$$\dot{\rho}_{00} = -\Gamma_0 \rho_{00} + \frac{i}{2}\left[\Omega_{R_1}\tilde{\rho}_{01} + \Omega_{R_2}\tilde{\rho}_{02} - \Omega_{R_1}\tilde{\rho}^*_{01} - \Omega_{R_2}\tilde{\rho}^*_{02}\right]$$

$$\dot{\rho}_{11} = \alpha_1\Gamma_0\rho_{00} - \Gamma_1\rho_{11} + \Gamma_{2\to 1}\rho_{22} + \frac{i}{2}\left[\Omega_{R_1}\tilde{\rho}^*_{01} - \Omega_{R_1}\tilde{\rho}_{01}\right]$$

$$\dot{\rho}_{22} = \alpha_2\Gamma_0\rho_{00} - \Gamma_2\rho_{22} + \Gamma_{1\to 2}\rho_{11} + \frac{i}{2}\left[\Omega_{R_2}\tilde{\rho}^*_{02} - \Omega_{R_2}\tilde{\rho}_{02}\right]$$

$$\dot{\tilde{\rho}}_{01} = -\left(\alpha_1\Gamma_0 + i\delta_{L1}\right)\tilde{\rho}_{01} + \frac{i}{2}\left[\Omega_{R_1}\left(\rho_{00} - \rho_{11}\right) - \Omega_{R_2}\tilde{\rho}_{21}\right]$$

$$\dot{\tilde{\rho}}_{02} = -\left(\alpha_2\Gamma_0 + i\delta_{L2}\right)\tilde{\rho}_{02} + \frac{i}{2}\left[\Omega_{R_2}\left(\rho_{00} - \rho_{22}\right) - \Omega_{R_1}\tilde{\rho}^*_{21}\right]$$

$$\dot{\tilde{\rho}}_{12} = -\rho_{12}\left(\Gamma_{12} + i\delta_R\right) + \frac{i}{2}\left[\Omega_{R_2}\tilde{\rho}^*_{01} - \Omega_{R_1}\tilde{\rho}_{02}\right]$$

Legend:

Γ_j – relaxation rate for state *j*.

Γ_{12} – decoherence rate.

$\Gamma_{j\to k}$ – collisional rate.

Ω_{Rk} – Rabi frequency.

α_k – Branching ratio.

Observing CPT

- In steady state, these six equations (Eqs. 11.1) can be numerically calculated or analytically solved [Orriols, 1979], yielding the CPT curves (right).

Normalized Values:

δ_{L1}	[-4, 4]	δ_{L2}	0
Γ_0	1	Ω_R	0.05
Γ_1, Γ_2	$5 \cdot 10^{-6}$	$\Gamma_{j \to k}$	$5 \cdot 10^{-6}$
Γ_{12}	$5 \cdot 10^{-6}$	α	1/2

The CPT curves: the steady-state excited population (ρ_{00}) plotted against different values for δ_R.

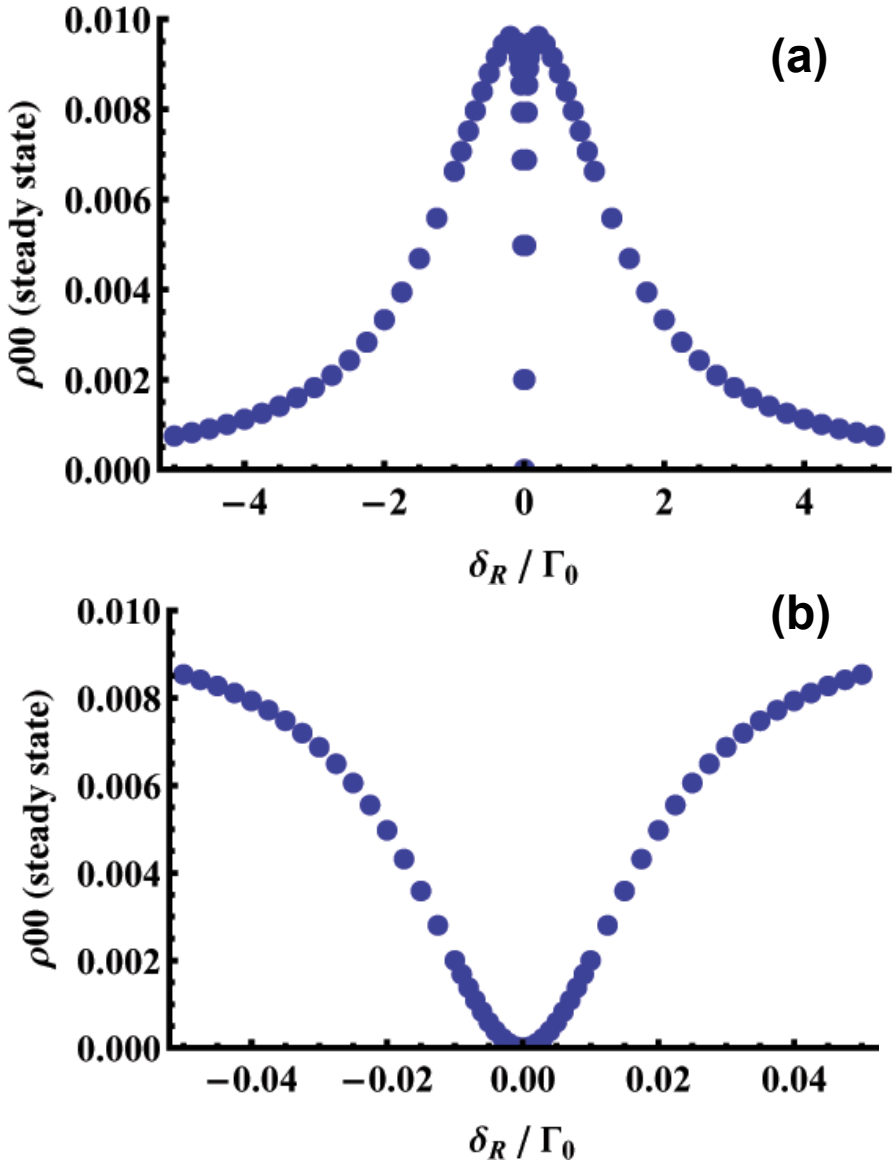

CPT Status

	Theory	Experiment
Gases (Na, Ne,Ar,Cs)	[1-4] and more…	[5-8] and more…
Cold Non-H plasmas	[9, 10]	[10]
Cold H plasmas	[11*, **12, 13**]	*none*
Warm H plasmas	[**13***]	*none*

* Peripherally

References:

1 – Arimondo E., and Orriols G. *Il Nuovo Cimento*, **17** 10 (1976).

2 – Orriols, G., *Il Nuovo Cimento*, **11** 1 (1979).

3 – Agap'ev B.D. *et al.*, *Phys. Uspekhi*, **36** 9 (1993).

4 – Arimondo E., *Progress in Optics,* **35** 257 (1996).

5 – Alzetta G. *et al.*, *Il Nuovo Cimento*, **36** 1 (1976).

6 – Vanier J., *et al.*, *Phys. Rev. A* **58** 3 (1998).

7 – Motomura K., *et al.*, *J. Opt. Soc. Am. B* **19** 10 (2002).

8 – Asahi H. *et al.*, *Opt. Lett.*, **28** 1153 (2003).

9– Harris, S.E. *Proc. Natl. Acad. Sci. USA* **94** 4853 (1997).

10 – Akhmedzhanov R. *et al.*, *Phys. Rev. E*, **69** 036409 (2004).

11 – Akhmedzhanov R. *et al.*, *Phys. of Plasmas* **14** 093505 (2007).

12 – Mitrani, J.M. *Senior Thesis*, 2009.

13 – Mitrani, J.M. *et al.*, 2009. *To Be Submitted…*

Sample CPT experiments

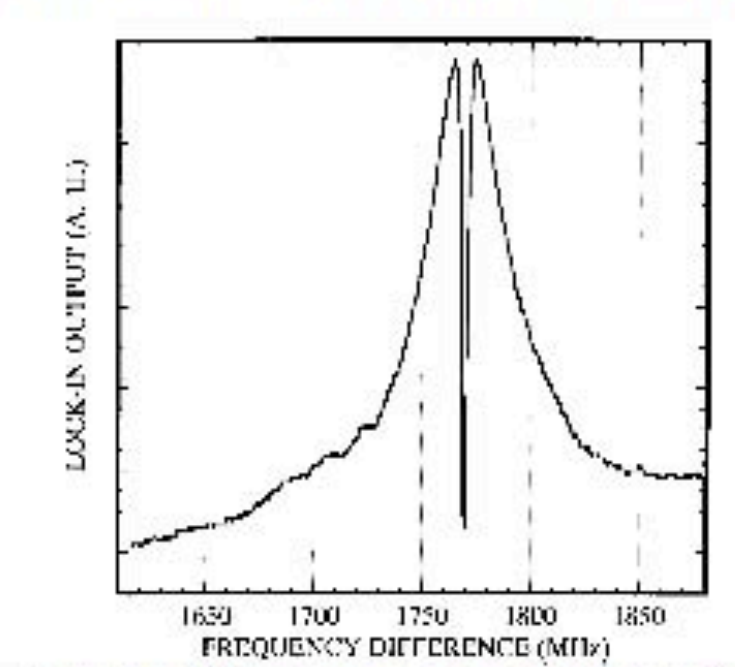

Na vapor: Motomura K., et al. (2002)

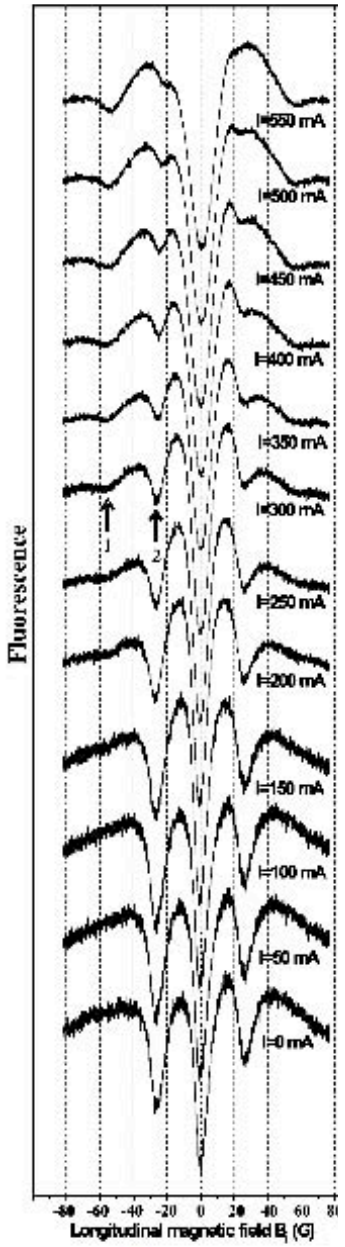

Ne plasma: Akhmedzhanov R., *et al.* (2004)

Outline

- Theory of coherent population trapping. How one can use CPT to measure **B**-fields in plasmas.
- Building an exhaustive model of CPT using the appropriate parameters from this experiment.
- Measuring fluorescence and the **B**-field from CPT effects.
- Clarifying assumptions, future experiments, and summary of results.
  - First extensive CPT model on hydrogen. (Isidor Rabi preferred working with hydrogen!)
  - First to show that CPT effects can be observed on the H_α line, even accounting for various spectroscopic complications.

Appropriate Parameters

- To model a CPT-based plasma diagnostic, one needs actual values for the parameters. (The previous plots used "artificial" parameters).
- The relevant values for the various rates will be derived from the PFRC plasma parameters, and from the H_α transition.

Rate	Value [Hz]	Normalized Value (Γ_0)	Comments	Cit
Γ_0	$2.25\cdot10^7$	1	Spontaneous decay from $3p_{1/2}$ state	[1]
Γ_1, Γ_2	8.23*	$3.66\cdot10^{-7}$*	Spontaneous decay from $2s_{1/2}$ state*	[1]
Ω_R	$6.84\cdot10^8$	30.4	$2\pi\cdot(a_0 e\cdot\mathbf{E}/h)$	
$\Gamma_{j\to k}$	~172	$7.64\cdot10^{-6}$	v_T/λ_{mfp}. $\lambda_{mfp} \sim T/pd^2$	[2]
Γ_{12}	$6.20\cdot10^6$	0.28	Decoherence rate: v_T/r	[3]
α_1, α_2	½	n/a	Equal decay probability	

* Stark-less.

Citations:

[1] – Ralchenko, Y. *et al.* "NIST Atomic Spectra Database," [online], 2008.

[2] – Lundberg, D. and S. Cohen. in *APS, 48th Ann. Meeting of the Division of Plasma Physics*, 2006.

[3] – Arimondo, E., *Phys. Rev. A* **54** 3 (1996).

CPT and Appropriate Parameters

- With the relevant parameters, one can numerically calculate the CPT curve.
- Two critical values are the FWHM, and $\Delta I_{\%}$, which measure the width and height of the "dip" respectively.
- The CPT curve is essential for measuring fluorescence (as will be described later).

Below: This is the CPT curve for the relevant parameters. Note when $\delta_R=0$, ρ_{00} doesn't completely deplete. The min. and max. values for ρ_{00} are .15 and .26 respectively. The values for the FWHM and $\Delta I_{\%}$ are $48\Gamma_0$ (1.08 GHz) and 43% respectively.

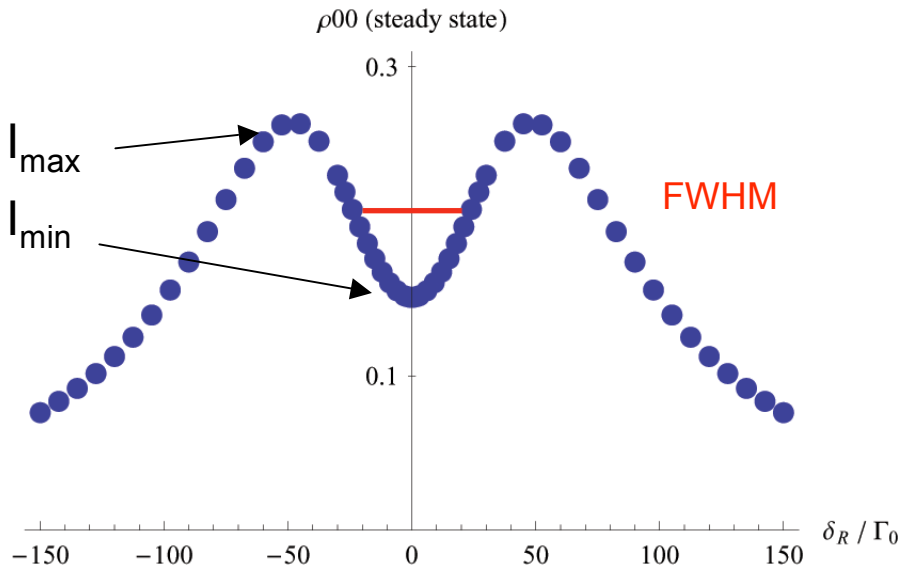

The H_α Emission Line

- The H_α emission (656 nm) is easily observed with standard optics. There are 7 degenerate electronic transitions, and 48 Zeeman-split electronic transitions (neglecting nuclear spin).
- With hyperfine splitting, there are 136 dipole transitions.
- The radiative intensity for each electronic transition depends on its decay rate, and the Clebsch-Gordan coefficients.
- Challenge: how to observe CPT effects in the presence of the 46+ other "non-target" transitions.

Legend:

1 – $3d_{3/2} \rightarrow 2p_{1/2}$.
2 – $3p_{3/2} \rightarrow 2s_{1/2}$.
3 – $3s_{1/2} \rightarrow 2p_{3/2}$.
4 – $3p_{1/2} \rightarrow 2s_{1/2}$.
5 – $3d_{5/2} \rightarrow 2p_{3/2}$.
6 – $3d_{3/2} \rightarrow 2p_{3/2}$.
7 – $3s_{1/2} \rightarrow 2p_{3/2}$.

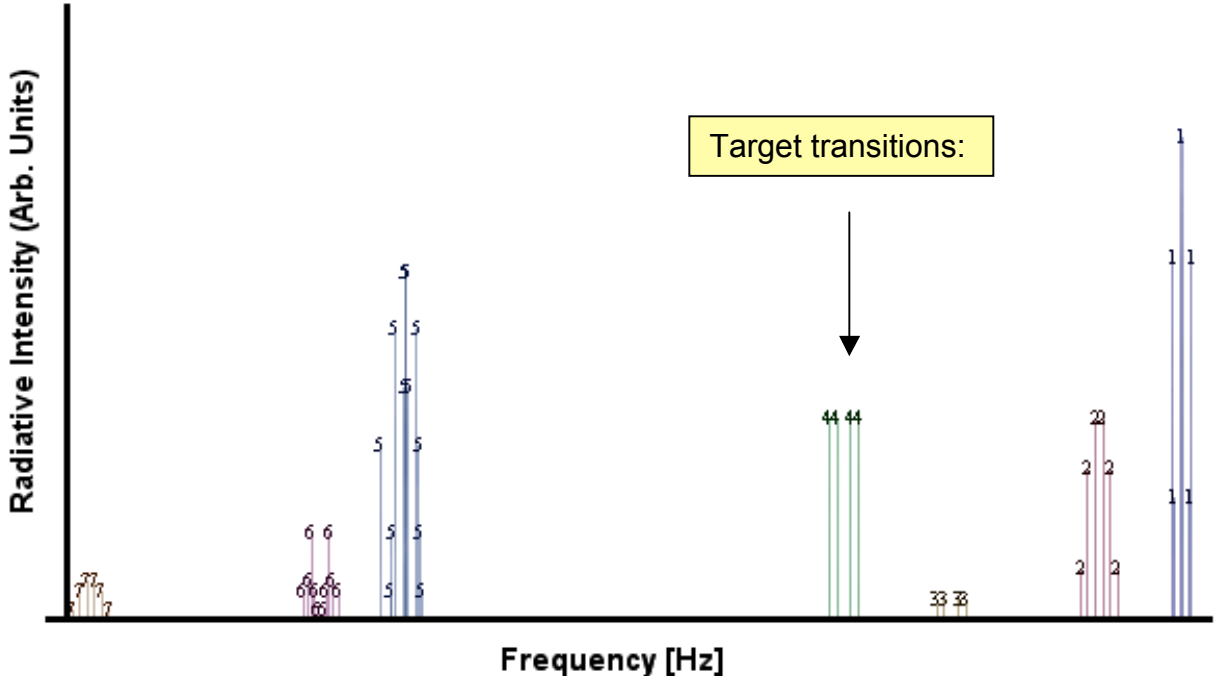

The H_α emission spectrum, with Zeeman splitting. The radiative intensity is based on the states' spontaneous decay rate and the Clebsch-Gordan coefficients.

H_α Energy Level Diagram

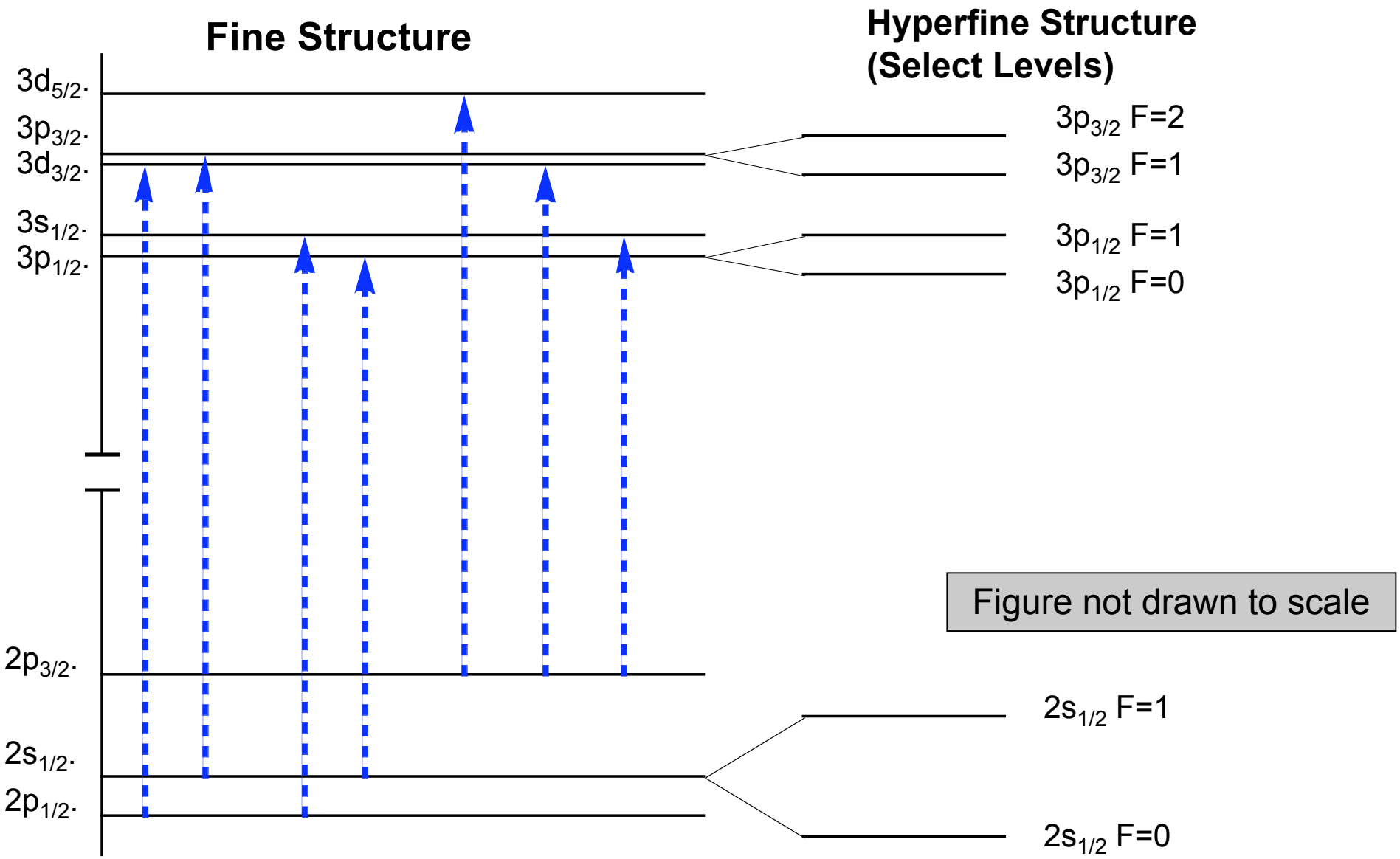

Angular Momentum Coupling

- Coupling between different angular momenta is critical, and depends on the **B**-field strength.
  - In the lower-level (n<4) states in hydrogen, the electron's orbital (**L**) and spin (**S**) angular momenta are coupled (**J**). The electron's total angular momentum (**J**) is further coupled the proton's spin momentum (**I**). The total angular momentum of the H atom is represented by **F**.
  - External magnetic fields can break the **I-J** and **L-S** coupling.

(Left): Figure showing **L-S** and **I-J** coupling, courtesy of [Herzberg, 1994].

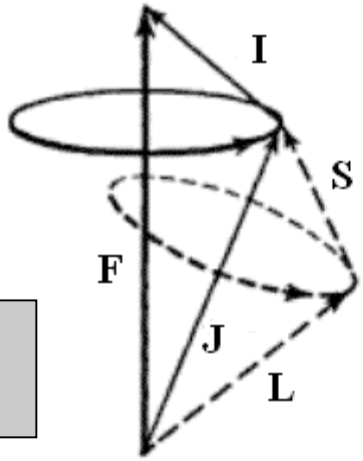

Fig. 70. Precession of the Angular Momentum Vectors about the Total Angular Momentum F for the Component $F = 5$ of a $^4F_4$ Term with $I = 2$. The solid-line ellipse shows the precession of I and J about F. The dotted-line ellipse shows the much faster precession of L and S about J, taking place at the same time.

Critical B-field values

Hyperfine Splitting			
State	Δν [MHz]	ΔE_{HF} ($\cdot 10^{-8}$) [eV]	B_{crit} [G]
$3d_{5/2}$:	2.71	1.13	1.94
$3p_{3/2}$:	7.03	2.91	5.02
$3d_{3/2}$:	4.22	1.75	3.02
$3s_{1/2}$:	52.77	21.86	37.70
$3p_{1/2}$:	17.59	7.29	12.57
$2p_{3/2}$:	23.74	9.83	16.96
$2s_{1/2}$:	178.07	73.74	127.23
$2p_{1/2}$:	59.36	24.58	42.41
Fine Splitting			
$3d_{5/2}$ vs. $3d_{3/2}$:	1,086	449.74	775.92
$3p_{3/2}$ vs. $3p_{1/2}$:	3,252	1346.74	2323.46
$2p_{3/2}$ vs. $2p_{1/2}$:	10,977	4545.85	7842.74

Weak* Field

B << B_{HF}. There is some splitting, but **J** and **I** are still coupled. The states can be defined in the {n,I,J,F,m_F} basis.

Strong* Field

B>>B_{HF}. Hyperfine splitting can be ignored, as **J** and **I** are no longer coupled. Each line is a doublet, due to nuclear spin. Basis is now {n,I,J,m_J,m_I}.

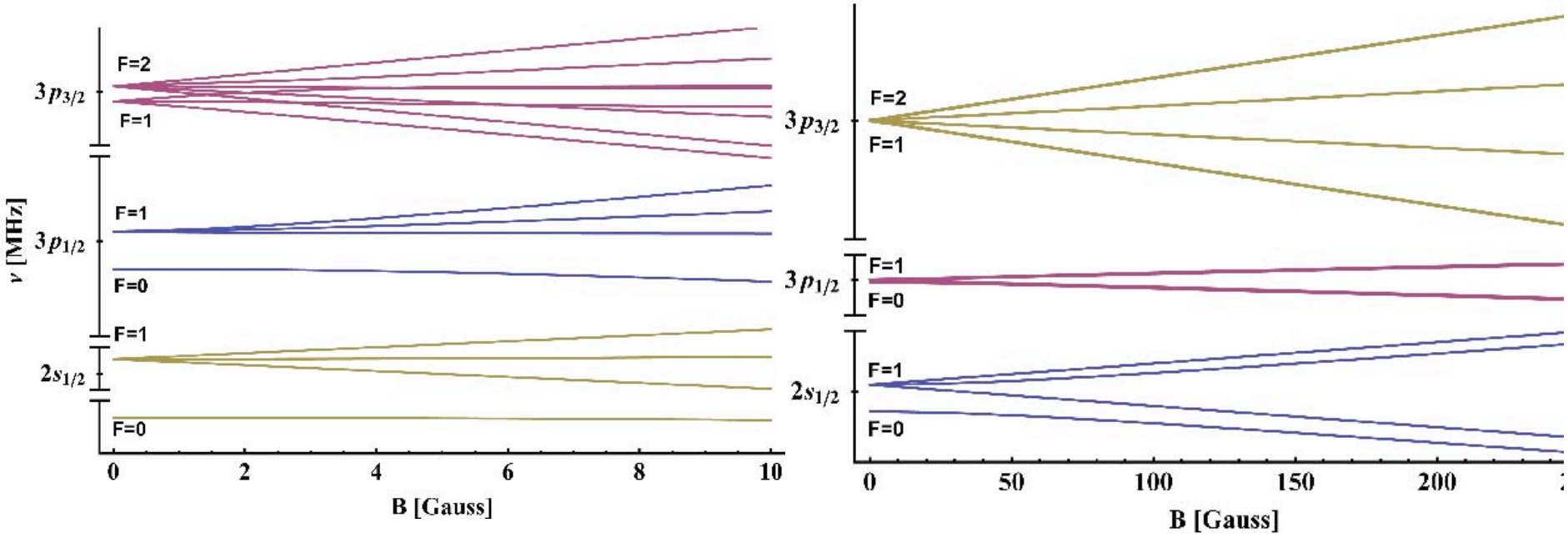

*Compared to hyperfine splitting

Stark Effect

- Stark effect arises due to **E**-fields.
  - In the PFRC, four **E**-fields are expected to arise – one is static (10 kV/m), and two are time-varying (1.5 and .3 kV/m) with frequencies of 14 and 0.1 MHz respectively. The fourth is pressure broadening.
  - Spatial locations and directions are important: E_r, E_z, E_ϕ.
- The Stark effect will shift and/or broaden the previous plots.
- Importantly, the Stark effect will "mix" the $2s_{1/2}$ and $2p_{1/2}$ states, destroying the metastability of the $2s_{1/2}$ state. But, with perpendicular **E** and **B** fields, the $2s_{1/2}$, m_J=+½ state remains relatively stable [1].
  - Initial experiments will be done to test the population of the $2s_{1/2}$ state.
  - These initial experiments may also be used to measure the **E** fields by fluorescence.

[1] – Bethe H. and Salpeter E., *Quantum Mechanics of One and Two-Electron Atoms*, Plenum/Roseta, 1977.

Line Broadening

- Doppler broadening dominates. It takes a Gaussian profile, and assumes a Maxwellian velocity distribution.
- Since the Doppler broadening profile is so wide, all H_α lines will be excited by the bichromatic laser – even though only two transitions are being targeted.

FWHM: ~22 GHz.

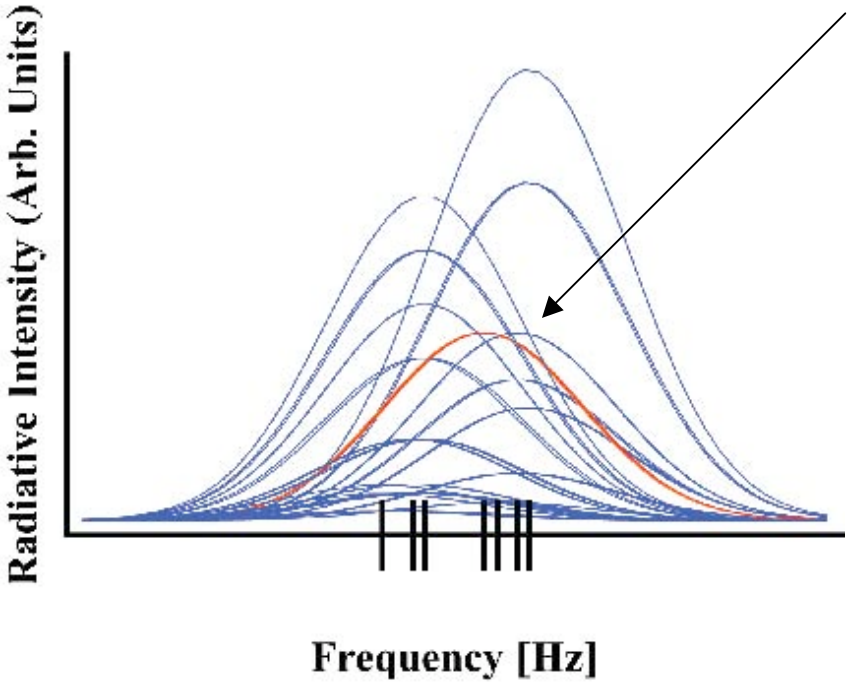

$$f_D(\upsilon) \propto \exp\left(-\frac{(\upsilon-\upsilon_0)^2}{2\sigma_D^2}\right)$$

$$\sigma_D = \upsilon_0 \mathrm{v}_T / c$$

The curves represent line profiles due to Doppler broadening. The red curves represent the $3p_{1/2} \rightarrow 2s_{1/2}$ transitions. The vertical black lines on the x-axis represent the mean frequencies for the seven fine transitions.

Outline

- Theory of coherent population trapping. How one can use CPT to measure **B**-fields in plasmas.
- Building an exhaustive model of CPT using the appropriate parameters from this experiment.
- Measuring fluorescence and the **B**-field from CPT effects.
- Clarifying assumptions, future experiments, and summary of results.
  - First extensive CPT model on hydrogen. (Isidor Rabi preferred working with hydrogen!)
  - First to show that CPT effects can be observed on the H_α line, even accounting for various spectroscopic complications.

H_α Emission Line - Intensities

- The background intensities for each Zeeman-split electronic transition can be calculated by [Sobelman, 1979]:

$$I_{ki} = S \frac{1}{4\pi} n_k \cdot A_{ki} \cdot h\upsilon_{ki}$$

Radiative Intensity

Clebsch-Gordan Coefficient

Solid Angle

Density*

(Assumed Coronal Equilibrium)

Spontaneous Decay Rate

Transition energy

*-This density doesn't account for the effects of laser pumping!

$$\frac{n_{3p}}{n_{1s}} = \frac{n_e < \sigma_{13} v >}{\sum A_{3j}}$$

Laser Pumping

- The excited state density should account for the effects of both laser pumping, and a Coronal equilibrium.
- To account for laser pumping, the radiative intensity for the $3p_{1/2}$ state should be:

$$I_{3i} \propto S \frac{1}{4\pi} \left(n_3^{coronal} + n_3^{pumping} \right) A_{ki} h\upsilon_k$$

Because the lasers are actively pumping atoms to the *n=3* states, one can show that $n_3^{pumping} >> n_3^{coronal}$

$$n_3^{pumping} \propto \rho_{00}(\delta_{L1})$$

The intensity will be proportional to the upper-state population [1].

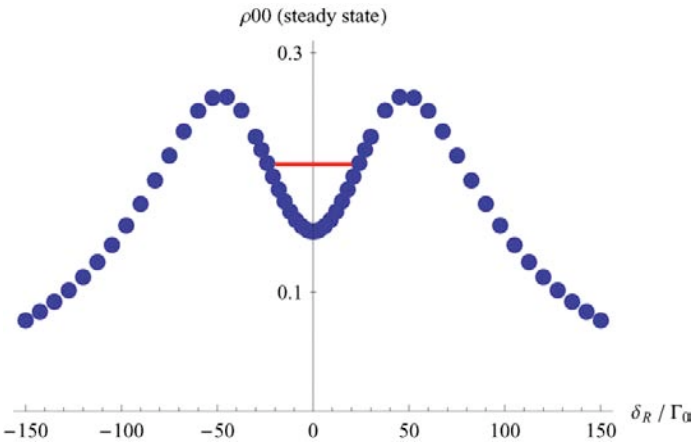

[1] - Arimondo, E., *Phys. Rev. A* **54** 3 (1996).

Ideal Fluorescent Intensity

- With no line broadening, only the two "target" transitions experience laser pumping from both lasers. This minimizes the effects of the other 46 "non-target" transitions.
- In fact, the ideal fluorescence intensity (right) is very similar.
  - For (**a**), δ_{L1} was scanned from $\pm 50\Gamma_0$ (± 1.1 GHz), and $\delta_{L2}=0$.
  - For (**b**), δ_{L1} was scanned from $\pm 200\Gamma_0$ (± 13.5 GHz), and $\delta_{L2}=0$.

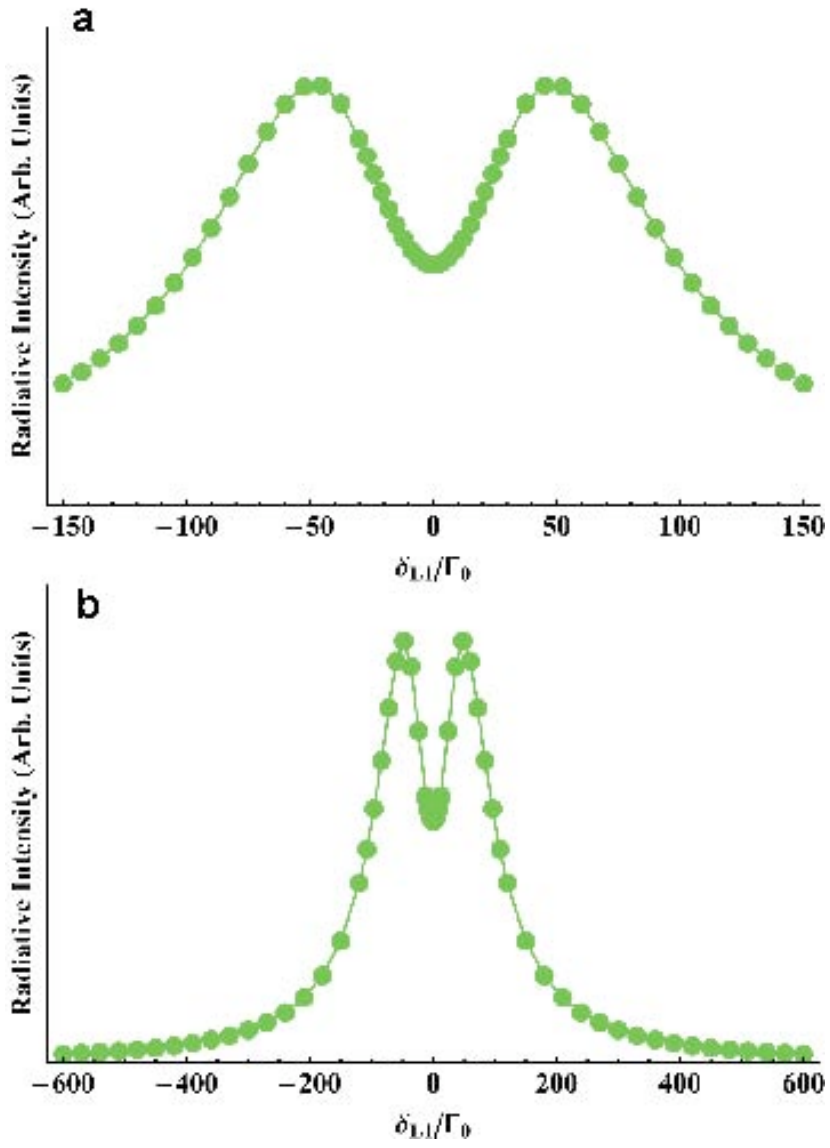

Values	ρ_{00} S.S.	Ideal Fluorescence
FWHM	~$48\Gamma_0$	~$48\Gamma_0$ (1.08 GHz)
$\Delta I_{\%}$	43%	43%

Two target transitions:

$3p_{1/2}$, $m=+½ \rightarrow 2s_{1/2}$, $m=+½$

$3p_{1/2}$, $m=+½ \rightarrow 2s_{1/2}$, $m=-½$

Effects of H_α Manifold

- Because of Doppler broadening, even though the lasers are tuned to the 2 "target" transitions, all 48 Zeeman-split electronic transitions will experience some interaction with the lasers.
  - However, not all interactions will be equal!
- Transitions with frequencies closer to the "target" transitions will experience larger laser interactions than transitions with frequencies further away.

Two target transitions:

$3p_{1/2}$, $m=+½ \rightarrow 2s_{1/2}$, $m=+½$

$3p_{1/2}$, $m=+½ \rightarrow 2s_{1/2}$, $m=-½$

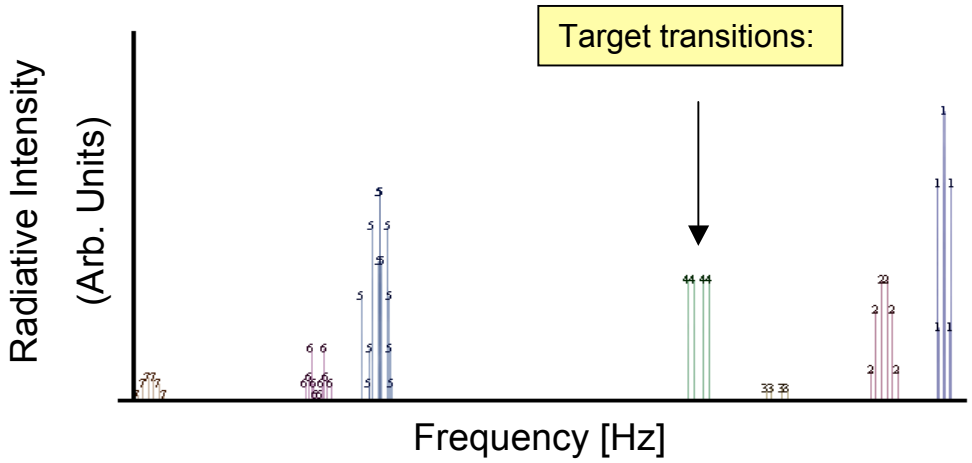

Effects of Doppler Broadening

- Since the states are "Doppler-broadened", they can be modeled as Gaussian profiles. Therefore, use a Gaussian profile to "diminish" the laser-state interactions.
  - This Gaussian profile is derived from the "Doppler-broadened" line profile for the $3p_{1/2}, m=+½ \rightarrow 2s_{1/2}, m=+½$ transition.

Original Fluorescence:

$$F(\delta_{L1}) \propto \frac{\int \rho_{00}(\delta_{L1}) \cdot I_{3i}^{Total}(\upsilon) \cdot B(\upsilon) d\upsilon}{\int B(\upsilon) d\upsilon}$$

$$I_{3i}^{Total}(\upsilon) = \sum_{q=1}^{48} \left[I_{3i}^{q} \cdot \delta(\upsilon - \upsilon_0^q) \right]$$

$$\alpha^q \propto \exp\left(\frac{(\upsilon^q - (\upsilon_0 + \delta_{L1}))^2}{2\sigma_L^2}\right)$$

$$f_D^q(\upsilon) \equiv \frac{1}{\sigma_D^q \sqrt{2\pi}} \exp\left(-\frac{(\upsilon - \upsilon_0^q)^2}{2(\sigma_D^q)^2}\right)$$

$$\sigma_D^q \equiv \upsilon_0^q \cdot v_T / c$$

$$I_{3i}^{DB}(\upsilon) = \sum_{q=1}^{48} \alpha^q \cdot I_{3i}^{q} \cdot f_D^q(\upsilon)$$

Modified Fluorescence:

$$F(\delta_{L1}) \propto \frac{\int \rho_{00}(\delta_{L1}) \cdot I_{3i}^{DB}(\upsilon) \cdot B(\upsilon) d\upsilon}{\int B(\upsilon) d\upsilon}$$

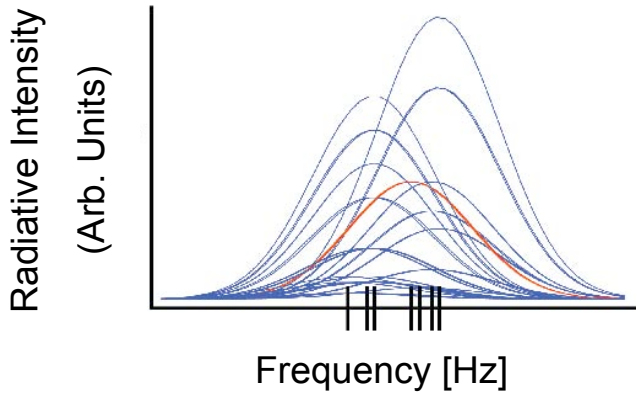

Effects of the Entire H_α Manifold

- To better account for all the Zeeman-split, H_α, electronic transitions, treat them as distinct Λ-systems, with distinct detuning parameters.
- Each transition experiences its own distinct detuning parameter, $\delta_{L1}{}^p$, and its own $\rho_{00}{}^p(\delta_{L1})$ term in the fluorescence equation.

$$F_{H\alpha}(\delta_{L1}^{0}) \propto \frac{\int\left\{\sum_{p=1}^{48}\left(\rho_{00}^{p}(\delta_{L1}^{p})\cdot\alpha_{p}\cdot I_{3i}^{p}\cdot f_{D}^{p}(\upsilon)\cdot B(\upsilon)\right)d\upsilon\right\}}{\int B(\upsilon)d\upsilon}$$

(Right): The effective resonance values for the two detuning parameters at resonance. $\delta_{L1}{}^p$ and $\delta_{L2}{}^p$ describe the detuning parameters for each of the 48 Zeeman transitions.

Effective Values Resonance for δ_{L1} and δ_{L2}				
Transition		δ_{L1}		δ_{L2}
Target	δ_{L1}^{0}	0	δ_{L2}^{0}	0
#1	δ_{L1}^{p}	-196	δ_{L2}^{p}	-183
#2	δ_{L1}^{p}	-149	δ_{L2}^{p}	-137
#3	δ_{L1}^{p}	-65	δ_{L2}^{p}	-53
#4	δ_{L1}^{p}	-2	δ_{L2}^{p}	+10
#5	δ_{L1}^{p}	+245	δ_{L2}^{p}	+258
#6	δ_{L1}^{p}	+293	δ_{L2}^{p}	+306
#7	δ_{L1}^{p}	+424	δ_{L2}^{p}	+436

Legend			
#1	$\|3d_{3/2}\rangle \rightarrow \|2p_{1/2}\rangle$	#2	$\|3p_{3/2}\rangle \rightarrow \|2s_{1/2}\rangle$
#3	$\|3s_{1/2}\rangle \rightarrow \|2p_{1/2}\rangle$	#4	$\|3p_{1/2}, m=-1/2\rangle \rightarrow \|2s_{1/2}\rangle$
#5	$\|3d_{5/2}\rangle \rightarrow \|2p_{3/2}\rangle$	#6	$\|3d_{3/2}\rangle \rightarrow \|2p_{3/2}\rangle$
#7	$\|3s_{1/2}\rangle \rightarrow \|2p_{3/2}\rangle$	**Target**	$\|3p_{1/2}, m=+1/2\rangle \rightarrow \|2s_{1/2}\rangle$

Effects of the Entire H_α Manifold

1

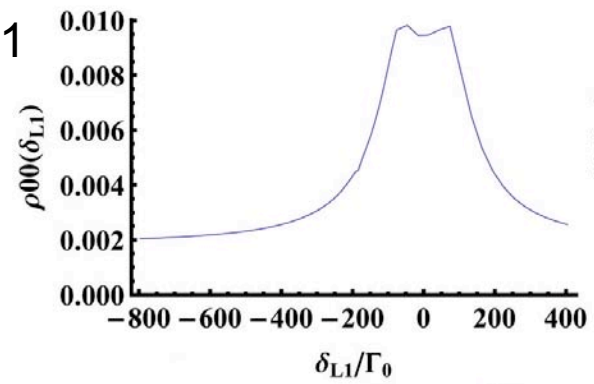

5

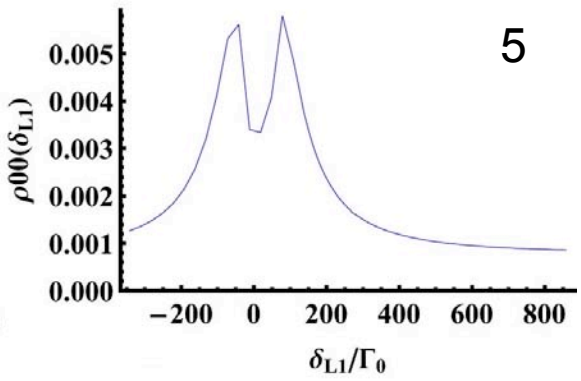

3

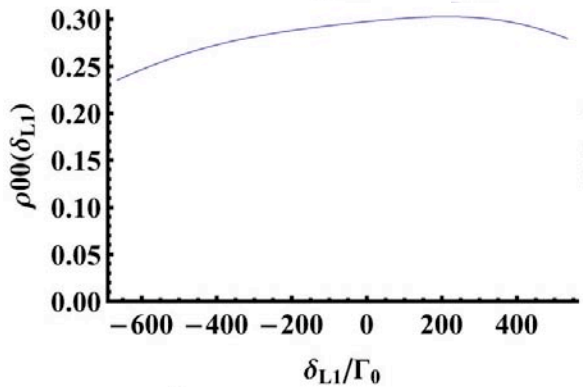

6

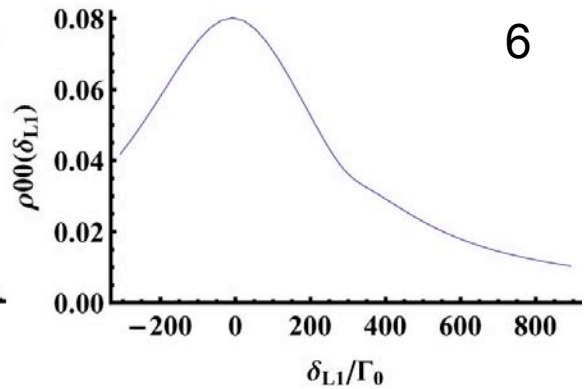

4

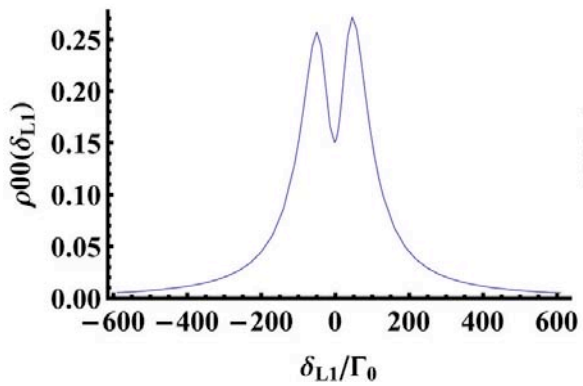

7

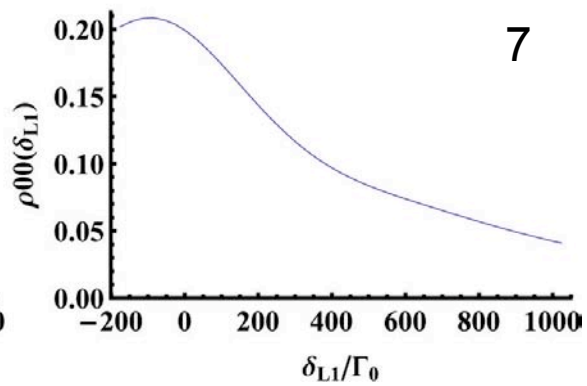

$\rho_{00}^{p}(\delta_{L1})$ terms for each fine transition:

m= –½

Legend:

1 – $3d_{3/2} \rightarrow 2p_{1/2}$.
2 – $3p_{3/2} \rightarrow 2s_{1/2}$.
3 – $3s_{1/2} \rightarrow 2p_{3/2}$.
4 – $3p_{1/2} \rightarrow 2s_{1/2}$.
5 – $3d_{5/2} \rightarrow 2p_{3/2}$.
6 – $3d_{3/2} \rightarrow 2p_{3/2}$.
7 – $3s_{1/2} \rightarrow 2p_{3/2}$.

2

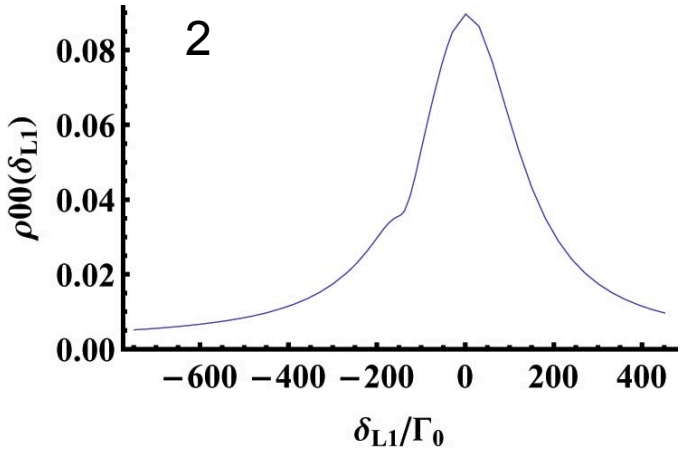

H_α Fluorescence Intensity

- Using Eq. (26.1) for the fluorescence resulted in different fluorescence intensities (right), where the CPT effects were less pronounced, and the minimum value for intensity was shifted.
- The green curves account for all seven degenerate transitions. The blue curves only account for the $n=3 \rightarrow 2s$ transitions, because the $2s$ state is metastable.

Values	Ideal Fluorescence	F1	F2
FWHM	~$48\Gamma_0$ (1.08 GHz)	~$48\Gamma_0$	~$48\Gamma_0$
$\Delta I_{\%}$	43%	33%	40%

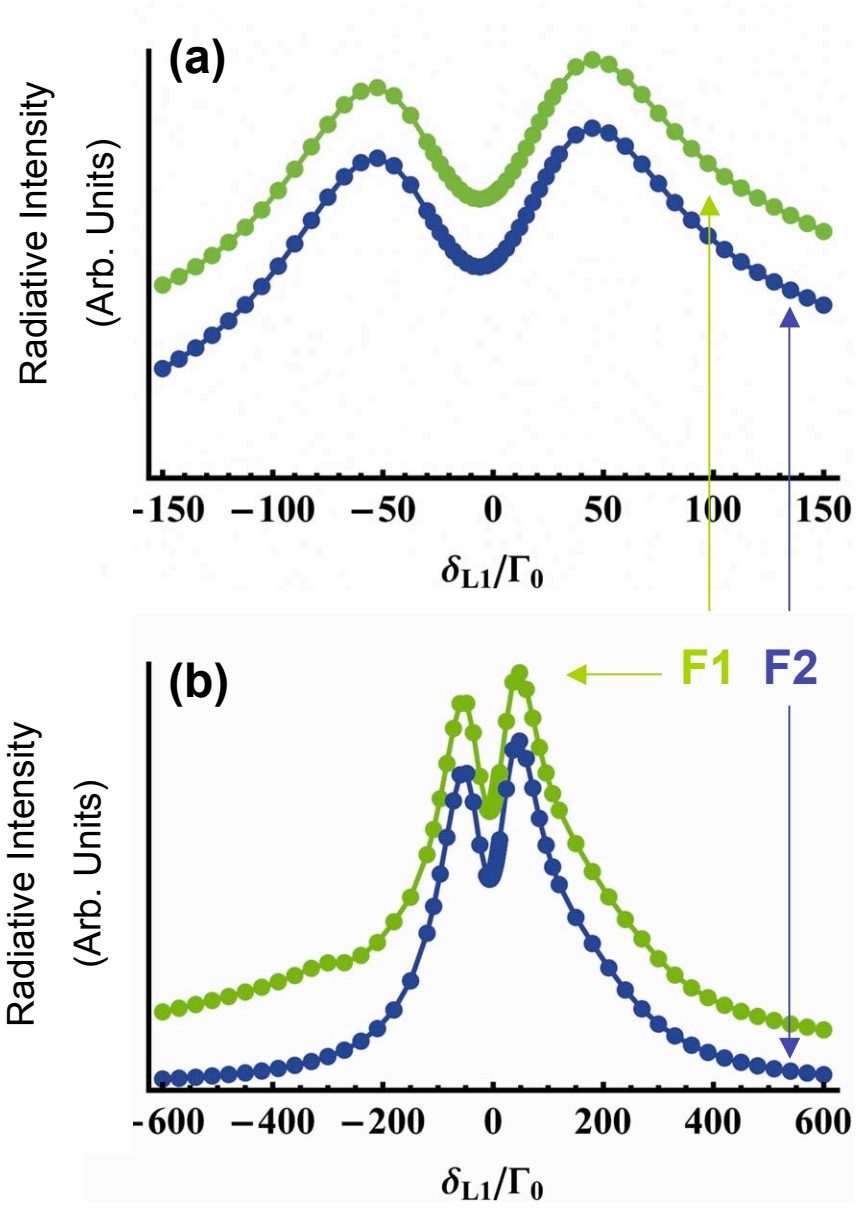

Magnetic Field Strength

- Measuring the magnetic field can in principle be done by looking at the fluorescence curves.
  - At the local minimum, $\delta_R=0$. Therefore, the only known parameters are the laser frequencies, ω_{Lk}, k={1,2}, and the frequency difference between the two lower states, ω_{12}.
  - Since the laser frequencies are known, one can solve for the magnetic field strength.
  - If the local minimum is shifted away from $\delta_R=0$, then more models of the fluorescence intensities are needed.
    - These models suggest that an external field of 100G shifts the minimum by $-6\Gamma_0$, or -135 MHz above the hyperfine splitting.

$$\delta_R = \omega_{L1} - \omega_{L2} + \omega_{12} \longrightarrow \omega_{12}(B) = \frac{g\mu_B B}{\hbar} + W_{HF}(B)$$

Magnetic Field Direction

- Measuring the magnetic field direction can be done by observing the polarization of the laser beams.
- A Λ-system can be constructed from either two σ-transitions ($\Delta m = \pm 1$), or a σ and a π-transition ($\Delta m = 0$).
- By observing the ratio of intensities of these two systems, one can derive an equation that gives the direction of the magnetic field [Akhmedzhanov, 2004].
  - Determining the field direction depends on the experimental setup.

Outline

- Theory of coherent population trapping. How one can use CPT to measure **B**-fields in plasmas.
- Building an exhaustive model of CPT using the appropriate parameters from this experiment.
- Measuring fluorescence and the **B**-field from CPT effects.
- Clarifying assumptions, future experiments, and summary of results.
  - First extensive CPT model on hydrogen. (Isidor Rabi preferred working with hydrogen!)
  - First to show that CPT effects can be observed on the H_α line, even accounting for various spectroscopic complications.

Clarifying Assumptions

- To apply a theoretical CPT model to measure **B**-fields in a plasma device using H_α emission, several assumptions were made.
  - A Λ-system could be constructed using the metastable $2s_{1/2}$ state.
  - We assumed that the plasma is in Coronal equilibrium, and that the light will easily penetrate the plasma.
  - To account for the effects of the 7 fine transitions, we assumed no interaction among the different $n=3$ states.
  - We didn't fully account for hyperfine or Stark effects. These effects were noted, and won't hamper our ability to observe CPT.
- A large (48x48) density matrix is needed to more accurately deal with each electronic transition in the H_α spectrum.

Progression of Experiments

- Initial experiments:
  - Observing H_α fluorescence in a steady cold unmagentized discharge.
  - Add a **B**-field, low β (e.g. helicon discharge).
  - Try to observe CPT effects.
  - Pulsed discharge.
  - RMF discharge.

CPT on the PFRC

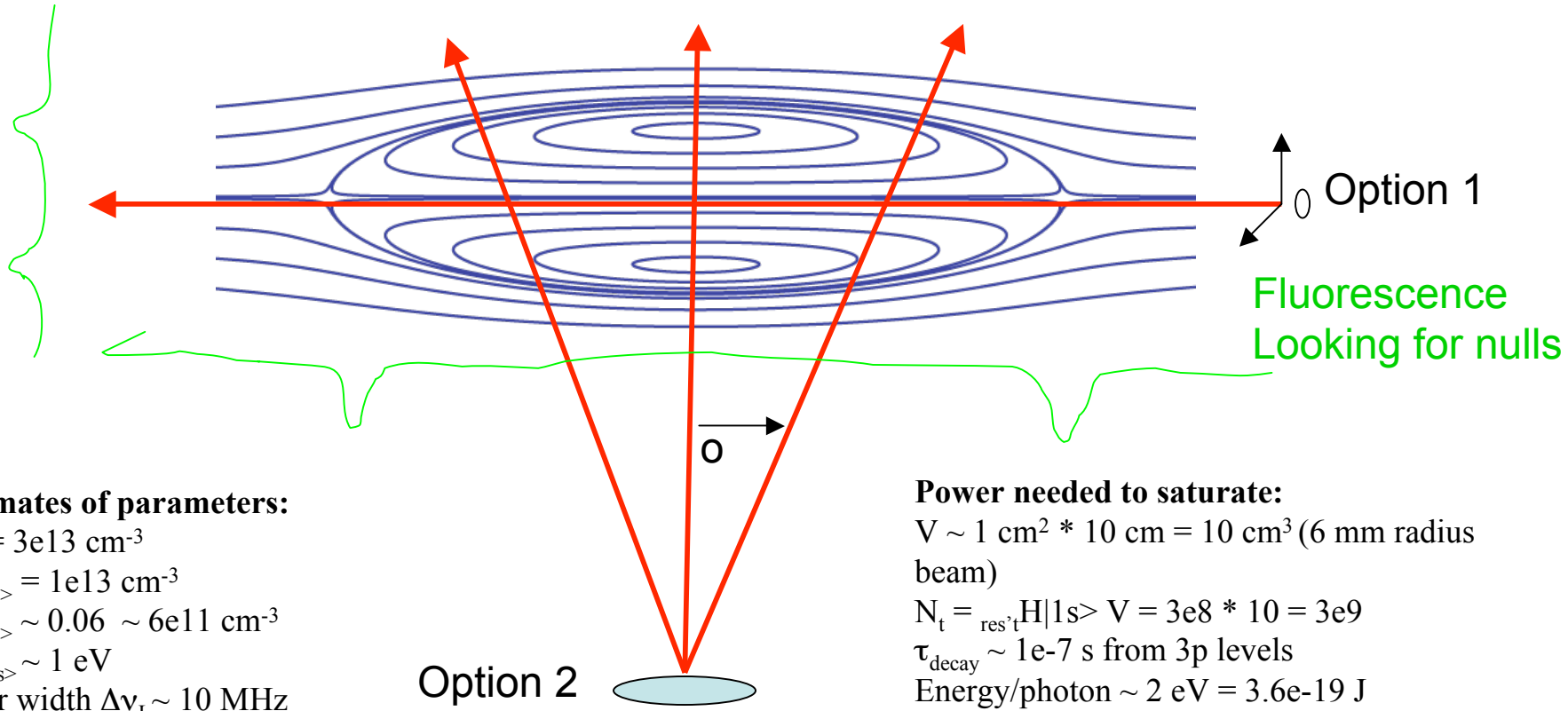

Estimates of parameters:

n_{H2} = 3e13 cm^{-3}

$n_{H1|1s>}$ = 1e13 cm^{-3}

$n_{H1|2s>}$ ~ 0.06 ~ 6e11 cm^{-3}

$T_{H1|2s>}$ ~ 1 eV

Laser width $\Delta\nu_L$ ~ 10 MHz

Doppler width $\Delta\nu_D$ ~ 20 GHz

Fraction of |2s> neutrals that are in resonance with laser = $\Delta\nu_L/\Delta\nu_D$ ~ 0.0005

Number density of resonant H|1s> ~ 0.0005 * 6e11 cm^{-3} = 3e8 cm^{-3}

Resonant photon absorption cross section: 0.7e-9 cm^2

Resonant (laser-produced Hα) photon mfp ~ 1/nσ ~ 1/(3e8*0.7e-9) ~ 4.7 cm

Power needed to saturate:

V ~ 1 cm^2 * 10 cm = 10 cm^3 (6 mm radius beam)

N_t = $_{res't}$H|1s> V = 3e8 * 10 = 3e9

τ_{decay} ~ 1e-7 s from 3p levels

Energy/photon ~ 2 eV = 3.6e-19 J

Laser power needed = 3e9 * 3.6e-19/1e-7 = 1e-2 W

Signal expected:

Solid angle collection optics: Ω ~ 1e-4

Photons from N_t in 1e-7 s: p_τ ~ 3e9

p_τ Ω ~ 3e9 * 1e-4 = 3e5. Plenty big!

3e3 photons/mm

With CPT contrast of 10% can resolve mm-sized dark regions to 3 std deviations.

Summary of Results

- Presented model of CPT in hydrogen.
  - Almost all previous studies used other atoms, such as Ne, or Na.
  - CPT in hydrogen poses a challenge with 48 Zeeman-split electronic transitions. (More if hyperfine splitting is included.)
  - This is the first model of CPT that accounts for all fine transitions in the H_α emission line.
- Showed that CPT effects can be observed in warm hydrogen plasmas with a weak magnetic field.
  - This paves the way for new experiments, and potentially new plasma diagnostics that can non-invasively measure the magnetic field in plasmas.

Select References

- Hugrass W., *J Plasma Phys.* **26** (1981).
- Shiokawa A. *et al.*, *Jap. J App. Phys.* **30** (1991).
- Milroy, R. *et al.*, *J Fusion Energy* **27** (1991).
- Orriols, G., *Il Nuovo Cimento*, **11** 1 (1979).
- Y. Ralchenko, A. Kramida, J. Reader, and NIST ASD Team, "NIST Atomic Spectra Database v3.1.5 [Online]." National Institute of Standards and Technology, Gaithersburg, MD. Available online at http://physics.nist.gov/asd3, 2008.
- D. Lundberg and S. Cohen, "Visible-wavelength emission by Hydrogen in the Princeton FRC," in American Physical Society, 48th Annual Meeting of the Division of Plasma Physics, October 30-November 3, 2006, abstract# QO2. 006, 2006.
- Arimondo, E., *Phys. Rev. A* **54** 3 (1996).
- Sobelman, I. *Atomic Spectra and Radiative Transitions*. Berlin, 1979.
- Akhmedzhanov R. *et al*, *Phys. Rev. E*, Vol. 69 036409 (2004).
- Herzberg, G. *Atomic Spectra and Atomic Structure*. Dover, 2007